A Deformable Object Model for Virtual Manipulation Based on Maintaining Local Shapes

Shinya MIYAZAKI, Junichi HASEGAWA

School of Computer and Cognitive Sciences, Chukyo University

Toyota City, Aichi Prefecture 470-0393, Japan

and

Takami, YASUDA*, Shigeki YOKOI**

***School of Informatics and Sciences, **Graduate School of Human Informatics, Nagoya University**

Nagoya City, Aichi Prefecture 464-8601, Japan

ABSTRACT

This paper proposes a new fundamental model of deformable objects for real-time and interactive applications. It is based on the mass-and-spring model, but in which the unit of elastic force definition for computation of dynamics is expanded from a spring to a volume element divided by the boundaries formed by mass-and-spring lattice. Displacements of the vertices of the volume element are defined to decide the elastic forces similar to the mass-and-spring model. Solving the equations of the equilibrium of internal force and moment of force derives them. As a result, proper elastic forces are operated for restoring the natural shape even if the object is rather soft and easily deformed, although they are becoming improper ones with the increase of displacement of the spring in mass-and-spring models. As the calculation is performed numerically and approximately, a method of reducing the approximation error is also presented.

Keywords: Elastic Object, Deformable, Real-time processing, Virtual manipulation, Computer Graphics.

1. INTRODUCTION

It is a general way for real-time and interactive simulation of deformable objects to establish equations of motion locally at every mass point in the mass-and-spring model and to solve them by the difference method [1,2]. It generates the state of objects at every point of constant time interval sequentially with a rather simple procedure. However, it has a serious problem the elastic force does not properly work for the restoration of the object deformation, especially in cases with objects that are rather soft and extremely deformable. As a result, divergence of oscillation or collapse of the goal of restoration occurs [3-5].

Roughly speaking, there are two reasons. The first reason being is that the elastic force is too simply defined. It is proportional to the displacement of the spring. It permits the amplitude of spring an infinite magnitude and leads the mass positions into disordered states. The phenomenon often appears when an external force operates along the same direction of the spring. Secondly, resultant force cooperated by multiple springs are not always suitable for the restoration of the object. It is reasonable that the mass-and-spring model imitates the molecular microstructure that fundamentally defines behaviors of real objects, but simple magnification does not perform properly. For example, when the object is extremely compressed and springs are closely parallel to each other, the elastic force almost does not operate along the vertical direction of the springs in spite of it being important to restoration. It is difficult to realize proper deformation with the spring-based force that acts only to keep a one-dimensional quantity of the natural length.

We have already proposed an improved model of springs in which the amplitude has constraints to less than the natural length of the spring [4]. It works well with the first reason. But, it is difficult only for the improvement of springs to solve the second reason because it depends on the competition among multiple springs.

In this time, we give a solution for it by expanding definition of the elastic force from a spring to a volume element that should be called a three dimensional spring. For example, if you imagine a cubic lattice as a fundamental structure, the unit of the volume element becomes each cube. The general procedure to define elastic forces is as follows. At first, unique equilibrium positions of the mass points (vertices) are decided in each element under the following conditions. They form the natural shape of the element and displacement vectors of them from the current positions corresponding to internal forces of the element that perform restoration phenomena. And then, a set of elastic forces is decided as being in proportion to the displacement vectors of the vertices. These procedures define proper forces for the restoration even if the object is extremely deformed. In the paper, a method of reducing the approximation error is also presented because the equilibrium positions of the vertices are numerically and approximately calculated.

Related Works

There have been some studies about the issue of the mass-and-spring model. Ref. 3 tries to avoid shrinking of the

elastic body by including a geometric constraint that keeps the volume of the object. It, however, does not always work as expected because it is merely a necessary condition for the shape restoration. And, a real object often performs deformations in which the volume changes.

Ref. 5 adopts the finite element method as in the definition of the stress. It, however, means that the application range is considerably limited. That is, the location of the object must be roughly fixed in the space and the degree of the deformation must be comparatively small.

2. MASS-AND-SPRING MODELS

In this section, the mass-and-spring model is explained, as it lays the foundation of the proposed model.

Definition of Force

Mass-and-spring model has the structure in which springs make trusses and mass points are placed in the nodes of the truss. If elastic forces and damping forces are chosen as the internal force and gravity is chosen as the external force, Eq (1) specifies the vector of force $\boldsymbol{F}_i$ operating on the node i. m_i is mass of the node i and $\boldsymbol{g}$ is the gravity constant. k_{ij}, L_{ij}, and D_{ij} are the elastic constant, natural length, and damping constant of the spring that is connecting the node i to node j. $\boldsymbol{p}_{ij}$ and $\boldsymbol{v}_{ij}$ are the relative position and relative velocity of the node i with respect to any node j which is connected to node i:

$$\boldsymbol{F}_i = m_i \boldsymbol{g} - \sum_j \left\{ k_{ij} \left(1 - \frac{L_{ij}}{|\boldsymbol{p}_{ij}|} \right) + D_{ij} \frac{\boldsymbol{v}_{ij} \cdot \boldsymbol{p}_{ij}}{\boldsymbol{p}_{ij} \cdot \boldsymbol{p}_{ij}} \right\} \boldsymbol{p}_{ij} \qquad (1)$$

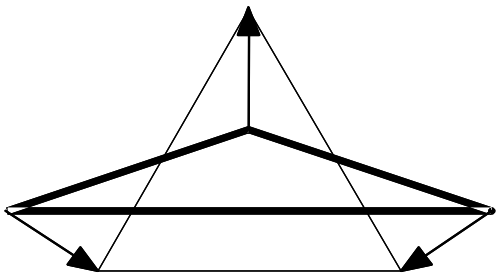

(a) Proper stresses for the shape restoration

(b) Stresses cooperated by three springs

Fig. 1 A set of stresses operating on a regular triangle deformed extremely.

The Method of Motion Generation

Difference equations of the dynamic equations of motion that are established locally in each node specify the velocity $\boldsymbol{V}_i(T)$ and position $\boldsymbol{P}_i(T)$ of the node i at discrete time T sequentially as:

$$\boldsymbol{V}_i(T + \Delta T) = \boldsymbol{V}_i(T) + \frac{\boldsymbol{F}_i(T)}{m_i} \Delta T \qquad (2)$$

$$\boldsymbol{P}_i(T + \Delta T) = \boldsymbol{P}_i(T) + \boldsymbol{V}_i(T) \Delta T \qquad (3)$$

Here, $\boldsymbol{F}_i(T)$ means the force operating on node i at time T. ΔT is the time step of evolution. Velocities and positions of nodes are renewed step by step in time. ΔT must be sufficiently small compared to the cycle of spring oscillation for the reliable simulation.

Collision Processing

The collision processing is also important to the motion generation. Here, a rebound of elastic objects is realized as a union of local rebounds of some nodes from a rigid surface. Every node that penetrates into the rigid region as a result of renewals in **2.2** is detected, and they are renewed extra with an ideal rebound from the rigid surface. Restitution coefficient between the node and the surface controls the global intensity

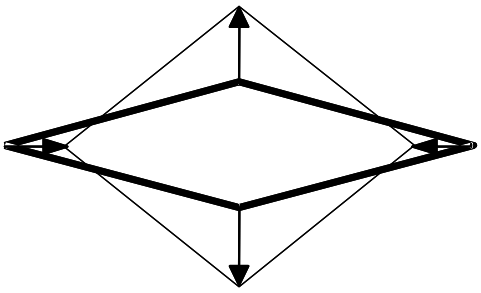

(a) Proper stresses for the shape restoration

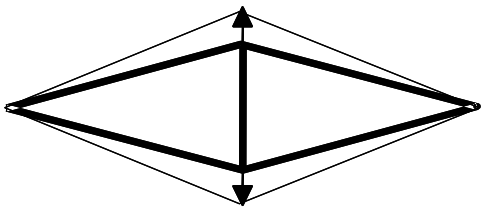

(b) A spring placed in the vertical diagonal

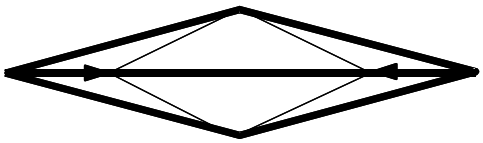

(c) A spring placed in the horizontal diagonal

Fig. 2 A set of stresses operating on a regular square deformed extremely.

of rebound. The reliability of this method comes from that the rebound process takes far smaller time than the cycle of elastic oscillation. The difference of the velocity of the node before and after the rebound is used to specify friction.

Although, only collisions between nodes and a surface are currently detected, they will be expanded to that between edges and a surface or that between faces and a surface.

3. SHAPE-BASED ELASTICITY

Mass-and-Spring Model and Proposed Model

In mass-and-spring models, the stress often becomes unexpected one for the shape restoration because of the competition among springs. Fig. 1(b), for example, shows a set of stress that is generated in a deformed regular triangle made of three springs. The stress operates as if the triangle drawn with bold lines is restored to the one drawn with thin lines (compare with Fig. 1(a)). Figs. 2(b) and 2(c) show another example in which five springs are placed in all of the edges and one of two diagonals of a regular square. The difference in the spring arrangement results the anisotropy of the stress.

Here, if the stress that restores the deformed shape to the natural one directly as shown in Figs. 1(a) and 2(a) is chosen, proper restoration may be expected. It is realized by modifying the definition of the stress in mass-and-spring models. For example, if the object consists of a cubic lattice, a set of stresses is defined at every cube, while a pair of stresses is defined at every spring in mass-and-spring models. Eq. (1) is expanded to Eq. (4) that specifies the vector of force $\boldsymbol{F}_i$ with elastic constant k_e and damping constant D_e of any elastic element e that includes node i. $\boldsymbol{d}_{ie}$ is the displacement of the node i with respect to its equilibrium position that is explained in the following sections. $\boldsymbol{v}_{ie}$ is the relative velocity of the node i with respect to the gravity velocity of the element e:

$$\boldsymbol{F}_i = m_i \boldsymbol{g} - \sum_e \{k_e \boldsymbol{d}_{ie} + D_e \boldsymbol{v}_{ie}\} \tag{4}$$

Definition of Equilibrium Shapes

It is appropriate to assume that both the resultant force and the moment of force of the stresses internally generated in each element are equal to the zero vectors. This specifies a unique equilibrium shape of the element. Eq. (5) expresses it with the relative vector $\boldsymbol{R}_i$ of the vertex i in the equilibrium shape and the relative vector $\boldsymbol{r}_i$ of the vertex i in the deformed shape with respect to the gravity of the element:

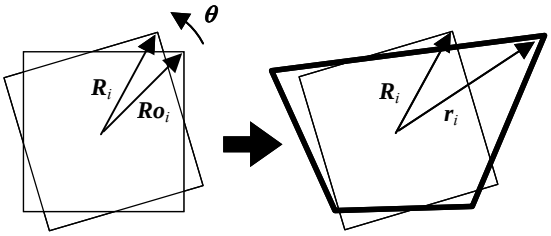

Fig. 3 An equilibrium shape of a polygonal element.

$$\sum_i \boldsymbol{r}_i \times k_e(\boldsymbol{R}_i - \boldsymbol{r}_i) = k_e \sum_i \boldsymbol{r}_i \times \boldsymbol{R}_i = \vec{0} \tag{5}$$

This specifies $\{\boldsymbol{R}_i\}$ when $\{\boldsymbol{r}_i\}$ is given. It also specifies $\{\boldsymbol{d}_{ie}\}$ in Eq. (4) as is equal to $(\boldsymbol{r}_i - \boldsymbol{R}_i)$.

In the implementation, the initial values of $\{\boldsymbol{R}_i\}$ are registered as $\{\boldsymbol{Ro}_i\}$, and $\{\boldsymbol{R}_i\}$ is defined as a result of the rotation of $\{\boldsymbol{Ro}_i\}$ around the gravity of the element. Then, Eq. (5) is replaced with Eq. (6) that specifies the rotation matrix M when $\{\boldsymbol{r}_i\}$ and $\{\boldsymbol{Ro}_i\}$ are given (Fig. 3):

$$\sum_i \boldsymbol{r}_i(T) \times M\boldsymbol{R}_i(T - \Delta T) = \vec{0} \tag{6}$$

Solution in Two-Dimensional Objects

The shape of the element is a polygon in the case of two-dimensional objects. If the object lies in the xy-plane, $\{\boldsymbol{Ro}_i\}$ and $\{\boldsymbol{r}_i\}$ are expressed as:

$$\boldsymbol{Ro}_i = \begin{pmatrix} X_i \\ Y_i \\ 0 \end{pmatrix}, \quad \boldsymbol{r}_i = \begin{pmatrix} x_i \\ y_i \\ 0 \end{pmatrix} \tag{7}$$

And, matrix M becomes the rotation matrix around the z-axis:

$$M = \begin{pmatrix} \cos\theta & -\sin\theta & 0 \\ \sin\theta & \cos\theta & 0 \\ 0 & 0 & 1 \end{pmatrix} \tag{8}$$

By substituting the variables in Eqs. (7) and (8) for Eq. (6), Eq. (9) is derived:

$$\frac{\sin\theta}{\cos\theta} = \frac{\sum_i (X_i y_i - Y_i x_i)}{\sum_i (X_i x_i + Y_i y_i)} \tag{9}$$

This specifies $\cos\theta$ and $\sin\theta$ when $\{\boldsymbol{Ro}_i\}$ and $\{\boldsymbol{r}_i\}$ are given. Successively, M and $\{\boldsymbol{R}_i\}$ are sequentially specified.

Solution in three-dimensional objects

Eq. (10) expresses matrix M in the case of three-dimensional objects with the unit vector of the rotation axis $\boldsymbol{u} = (u_x, u_y, u_z)$ and the rotation angle θ [6]:

$$M = \boldsymbol{u}\boldsymbol{u}^{\mathrm{T}} + \cos\theta(I - \boldsymbol{u}\boldsymbol{u}^{\mathrm{T}}) + \sin\theta \begin{pmatrix} 0 & -u_z & u_y \\ u_z & 0 & -u_x \\ -u_y & u_x & 0 \end{pmatrix} \tag{10}$$

Here, $u_x^2 + u_y^2 + u_z^2 = 1$ is satisfied.

As it is impossible to specify $\boldsymbol{u}$ and θ by solving Eq. (6) analytically, the approximate values of them are obtained. If $\{\boldsymbol{R}_i\}$ at time $(T - \Delta T)$ is adopted as $\{\boldsymbol{Ro}_i\}$ in Eq. (6), Eq. (6) is replace with Eq. (11):

$$\sum_i \boldsymbol{r}_i \times M\,\boldsymbol{Ro}_i = \vec{0} \tag{11}$$

Then, a condition of approximation that θ is nearly equal to zero may be applied. By substituting the equations $\cos\theta = 1$ and $\sin\theta = \theta$ for Eq. (10), matrix M is simplified as:

$$M = \begin{pmatrix} 1 & -u_z\theta & u_y\theta \\ u_z\theta & 0 & -u_x\theta \\ -u_y\theta & u_x\theta & 1 \end{pmatrix} \tag{12}$$

When $\{\boldsymbol{R}_i(T-\Delta T)\}$ and $\{\boldsymbol{r}_i(T)\}$ are given as:

$$\boldsymbol{R}_i(T-\Delta T) = \begin{pmatrix} X_i \\ Y_i \\ Z_i \end{pmatrix}, \quad \boldsymbol{r}_i(T) = \begin{pmatrix} x_i \\ y_i \\ z_i \end{pmatrix} \tag{13}$$

Eq. (11) is expanded as:

$$\sum_i \begin{pmatrix} -u_y\theta X_i y_i + u_x\theta Y_i y_i + Z_i y_i - u_z\theta X_i z_i - Y_i z_i + u_x\theta Z_i z_i \\ X_i z_i - u_z\theta Y_i z_i + u_y\theta Z_i z_i + u_y\theta X_i x_i - u_x\theta Y_i x_i - Z_i x_i \\ u_z\theta X_i x_i + Y_i x_i - u_x\theta Z_i x_i - X_i y_i + u_z\theta Y_i y_i - u_y\theta Z_i y_i \end{pmatrix} = \begin{pmatrix} 0 \\ 0 \\ 0 \end{pmatrix} \tag{14}$$

It is rearranged by the variables u_x, u_y, u_z, and θ into:

$$\theta \begin{pmatrix} \sum_i Y_i y_i + \sum_i Z_i z_i & -\sum_i X_i y_i & -\sum_i X_i z_i \\ -\sum_i Y_i x_i & \sum_i Z_i z_i + \sum_i X_i x_i & -\sum_i Y_i z_i \\ -\sum_i Z_i x_i & -\sum_i Z_i y_i & \sum_i X_i x_i + \sum_i Y_i y_i \end{pmatrix} \begin{pmatrix} u_x \\ u_y \\ u_z \end{pmatrix} = \begin{pmatrix} \sum_i Y_i z_i - \sum_i Z_i y_i \\ \sum_i Z_i x_i - \sum_i X_i z_i \\ \sum_i X_i y_i - \sum_i Y_i x_i \end{pmatrix} \tag{15}$$

It specifies the ratio of $u_x : u_y : u_z$. Successively, $\boldsymbol{u}$ and θ are sequentially specified. Finally, $\{\boldsymbol{R}_i(T)\}$ is specified as:

$$\boldsymbol{R}_i(T) = M\boldsymbol{R}_i(T-\Delta T) = \begin{pmatrix} X_i - u_z\theta Y_i + u_y\theta Z_i \\ u_z\theta X_i + Y_i - u_x\theta Z_i \\ -u_y\theta X_i + u_x\theta Y_i + Z_i \end{pmatrix} \tag{16}$$

Experiments

The proposed model is compared with the mass-and-spring model to confirm the advantage. In Fig. 4, the upper figures and lower figures show scenes of dynamic simulation of the proposed model and the mass-and-spring model, respectively. It can be often seen in mass-and-spring model that some of the elements turn over because of insufficient stresses. In the

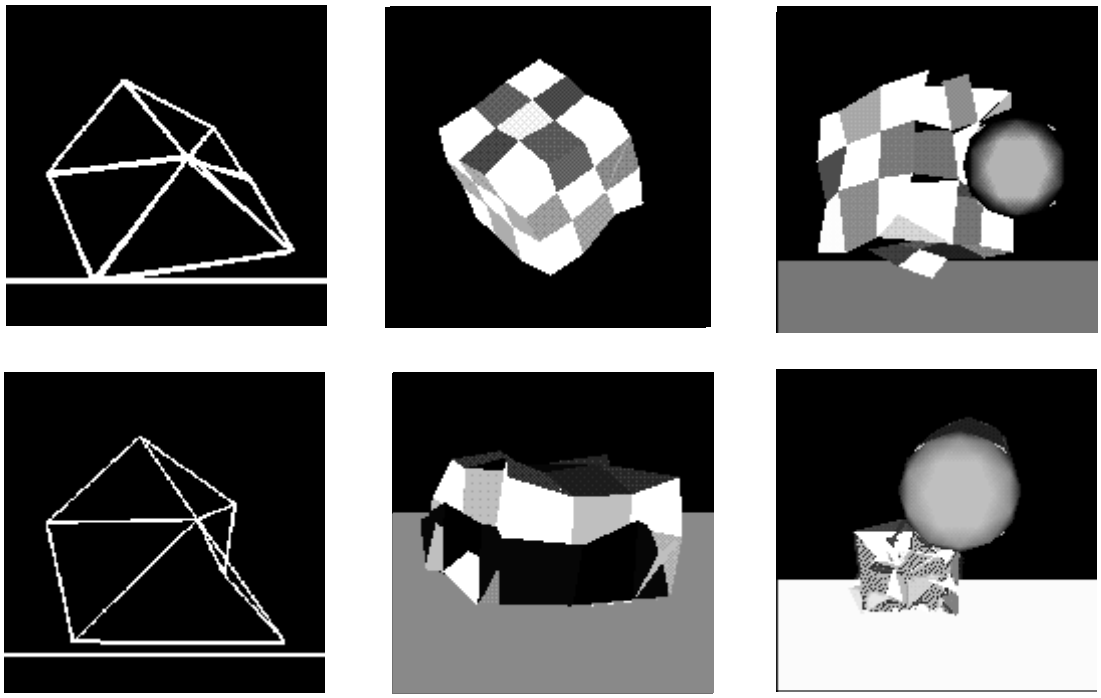

(a) $k/m = 10^4$ (b) $k/m = 10^4$ (c) $k/m = 10^5$

Fig. 4 Comparisons between the proposed model (upper) and the mass-and-spring model (lower).

example of a two-dimensional object consisting of six triangles, the triangle that has the largest obtuse angle is easily turning over (Fig. 4(a) lower). In the example of a three dimensional object consisting of 3 X 3 X 3 cubic elements, large forces received from the floor turn over all the elements in the nearest row to the floor (Fig. 4(b) lower). When the ratio of elastic constant k to mass m that means the strength of elasticity is increased to 10^5, the problem has not appeared even in mass-and-spring models. It, however, appears again when larger forces received from the manipulator operate. The object is shrinking as a result of the repeated collision with the manipulator (Fig. 4(c) lower).

4. REDUCTION OF APPROXIMATION ERRORS

Solutions of equilibrium shapes include approximation errors in three-dimensional objects. In this section, the influence of the errors to the result of dynamic simulation is evaluated and a method to decrease the errors is presented.

Evaluation of Errors

As approximation errors occur at the rotation axis $\boldsymbol{u}$ and the rotation angle θ in subsection **3.5**, they result as if an extra force that rotates the element operated. Therefore, acceleration of angle performed by the extra force is chosen as the criterion for evaluation. If a rough value of the moment of inertia of the element I is permitted:

$$I = \sum_i m_i \left| \boldsymbol{Ro}_i \right|^2 \tag{17}$$

Acceleration of angle α is equal to the moment of force divided by I:

$$\alpha = \frac{k_e \sum_i \boldsymbol{r}_i \times \boldsymbol{R}_i}{I} \tag{18}$$

Row A in Table 1 shows average $\mu(\alpha)$, standard deviation $\sigma(\alpha)$, and maximum max (α) of the acceleration of angle α for 10 seconds from the moment when a single cubic element collides with the floor for the first time after falling from ten times the height of the size of the cube. Three kinds of values 10^4, 10^5, and 10^6 that are comparatively realistic ones [4] are assigned to k/m. The value of ΔT is fixed at 1/10 of the cycle of elastic oscillation in each case, which is small enough to succeed dynamic simulation. In row B in which ΔT is fixed at 1/100, the influence of approximation errors are smaller than in row A, because the value of θ approaches zero with the decrease of ΔT. Computation time, however, increases with the inverse proportion to ΔT.

Reduction of Errors

The approximation values of $\{\boldsymbol{R}_i(T)\}$ derived in subsection **3.5** are not certainly the true ones, but they are at least nearer to the true ones than $\{\boldsymbol{R}_i(T-\Delta T)\}$; the derived $\{\boldsymbol{R}_i(T)\}$ is more desirable $\{\boldsymbol{Ro}_i\}$ than $\{\boldsymbol{R}_i(T-\Delta T)\}$. Therefore, it is considered that the procedure of solving Eq. (6) one time brings the approximation value of $\{\boldsymbol{R}_i\}$ closer to the true one. In other words, the iteration of solving Eq. (6) converges $\{\boldsymbol{R}_i\}$ into the true solution with an initial value $\{\boldsymbol{R}_i(T-\Delta T)\}$.

Table 1 The evaluation values of approximation errors.
- means below lower limit of the measurable range.

$k/m = 10^4$

	A	B	C	D
number of iteration	1	1	2	3
ΔT	0.006	0.0006	0.006	0.006
$\mu(\alpha)$	4.52554	0.032915	0.000493	-
$\sigma(\alpha)$	4.49862	0.037503	0.00211	-
max(α)	30.87597	0.320008	0.060352	0.000001

$k/m = 10^5$

	A	B	C	D
number of iteration	1	1	2	3
ΔT	0.002	0.0002	0.002	0.002
$\mu(\alpha)$	1.987712	0.030974	-	-
$\sigma(\alpha)$	1.68312	0.028445	0.000001	-
max(α)	9.119262	0.157926	0.000017	-

$k/m = 10^6$

	A	B	C	D
number of iteration	1	1	2	3
ΔT	0.0006	0.00006	0.0006	0.0006
$\mu(\alpha)$	1.301888	0.005511	-	-
$\sigma(\alpha)$	1.297613	0.005129	-	-
max(α)	7.570902	0.034552	-	-

Rows C and D in Table 1 show results in which the number of iteration is fixed at two and three, respectively, and ΔT is fixed at the same value as in Row A. The influence of approximation errors is far smaller than in Row B that relies on the reduction of ΔT, and the rotate of the element performed by the approximation errors is usually constrained by the elements connected around. Therefore, the number of iteration may be fixed at two in practice. Then, the computation time of the proposed model is proportional to the number of elements as well as the mass-and-spring models. In the experiment, the ratio of computation time of the proposed model to that of the mass-and-spring model was 1.05.

5. CONCLUSIONS

We have proposed a deformable model in which proper stresses operate for the shape restoration. It is just the solution of the issue of mass-and-spring models mentioned in the beginning of this paper.

In the mass-and-spring model, the shape of the element is difficult to be varied because the arrangement of springs must be changed depending on it. On the other hand, the proposed model permits an arbitrary shape of the element. That is also of great advantage in practical applications that necessarily handle free form objects.

Acknowledgments. The authors would like to thank Professor Teruo Fukumura of Chukyo University for his encouragement and assistance. This research was supported in part by the

grant-in-aid for Private University High-Tech Research Center from the Ministry of Education, Japan.

REFERENCES

[1] D.Terzopoulos, J.Platt, A.Barr, and K.Fleisher. Elastically Deformable Models. Computer Graphics, 21(4), pp.205-214, 1987.

[2] A.Norton, G.Turk, B.Bacon, J.Gerth, and P.Sweeney. Animation of Fracture by Physical Modeling. The Visual Computer, 7, pp.210-219, 1991.

[3] M.Terasawa and F.Kimura. Volume Preserving Deformation Technique for Dynamic Computer Animation. IPSJ, CG Symposium Proc., pp.177-184, 1992.(in Japanese)

[4] S.Miyazaki et al. Modeling and Implementation of Elastic Object Manipulation in Virtual Space. Electronics and Communications in Japan, Part 3, 81(4), 1998.

[5] K.Hirota and T.Kaneko. A Study on the Model of an Elastic Virtual Object. Trans. SICE, 34(3), pp.232-238, 1998. (in Japanese)

[6] J.Neider, T.Davis, and M.Woo. OpenGL Programming Guide. Addison-Wesley, p.478, 1993